1 of 1

LA-UR -94-206

CONF-940756--2

Los Alamos National Laboratory is operated by the University of California for the United States Department of Energy under contract W-7405-ENG-36

TITLE Percolation, Wave Propagation, And Void Link Up Effects in Ductile Fracture

AUTHOR(S) D. L. Tonks

SUBMITTED TO EURO DYMAT 94, Oxford, England, Sept 1994

DISCLAIMER

Los Alamos National Laboratory
Los Alamos, New Mexico 87545

FORM NO 836 R4
ST NO 2629 5 81

PERCOLATION, WAVE PROPAGATION, and VOID LINK-UP EFFECTS IN DUCTILE FRACTURE

D. L. Tonks (Applied Theoretical Division, LANL)

Abstract - This work investigates the time evolution and spatial morphology of ductile damage based on void growth and coalescence. The size enhancement of damage cluster growth, as well as wave speed limiting of growth, are treated microscopically. Simplified 2D plane strain simulations using individual voids are done with uniaxial stress and explained with a probabilistic theory. At low strain rates, fracture occurs by long, localized cracks. At high strain rates, widespread, random damage breaks the system. The Voronoi tessellation of voids can be used to map out the spatial network of still solid material in 3D ductile fracture. Using it, the spallation porosity is calculated based on percolation theory.

Introduction

On the microscopic scale, high strain rate ductile fracture is due to the nucleation, growth, and link up of voids. The spatial ordering of this process depends on the initial ordering of the voids and how the voids link up. We explore the above effects through model 2D and 3D simulations and analytical modeling of the results. Wave speed limiting of void link-up is approximately included. It is shown that a disordered initial void configuration gives rise to spatially disordered breaking at high strain rates, where wave propagation times limit the range over which voids can communicate with each other. The sample breaks due to the general build up of wide spread damage until percolation occurs. At low strain rates, for applied uniaxial strain, the ductile damage consists of long, ordered, "crack-like" clusters. This is because, when voids link up into a cluster, there is time for the enhanced stress and strain fields to form at their boundaries, which extends the cluster's void link up range. In this case, the sample breaks with little general damage, when the longest crack rapidly outstrips is neighbors. Consequently, the strain to fracture in the low strain rate case is significantly less than in the high strain rate case.

Roughly speaking, the wave speed limiting of void linking is treated by delaying the enhancement in strain fields at the void cluster boundary by the time for a sound wave to transit the cluster. This delay is similar to the one seen in the stress intensity factor of growing brittle cracks. The two situations should be similar since, in both cases, the enhanced range is due to elastic release waves.

Inertia effects of void growth are not included but they have been shown to be negligible for typical void sizes and driving strain rates.[1] Inertia is included in the retardation of void linking due to wave propagation.

The simulation results show changes in the void cluster population, with cluster growth, from exponential to a power law. There is a power law relating the damage at breaking to system size, and a more complicated size effect of the strain to fracture.

Analytical models have been formulated to explain the point of fracture in the 2D simulations. At high strain rates, the wave speed limited regime is explained with random percolation theory. The organized clusters at low strain rates are explained using an integral equation for cluster growth.

The spallation calculation using the Voronoi tessellation is based on the network of still solid mate-

rial. The earlier practice of using the porosity at which random voids percolate (30%) is not accurate because the solid connecting network still exists at this point.

Void Linking

In order to form a continuous internal surface that separates the sample, the growing voids must come together in some way, or coalesce. We will use the term void linking here. In dynamic situations, this will occur when the intervoid ligament undergoes a mechanical localized instability that rapidly thins out the ligament in a localized region at the expense of an unloading and reduction of deformation in the surroundings.[2-4] Various instability modes are possible. We assume only that some sort of localized flow quickly destroys the stress carrying ability of the intervoid ligament when the instability is triggered. We make the approximation that the loss of strength happens instantaneously. In reality, some local straining occurs first, at a rate greatly amplified by the linking instability. For example, for the quasi static case, Thomason[2] envisions a whole sheet of voids whose intervoid ligaments undergo flow localization all at once. He states that, in this case, the elastic loading extends all the way to the sample boundaries, so that most of the sample straining gets dumped into the very narrow linking void sheet, which then breaks almost instantly with very little additional macroscopic strain. We are using this same general idea here, but on a local scale.

To model void linking, the triggering conditions must be known. We will make the approximation that the linking triggers when voids are closer than a certain distance. We will give each void a linking range such that when the ranges of two voids overlap, the ligament necking process is triggered. The range of a spherical void is roughly the size of its diameter.[2] Thomason has justified this sort of modeling for the quasistatic situation with slip line fields and instability theory in both two and three dimensions.[2-4]

We have also added the effect of voids first linking up locally into local units which then further link up. It is apparent that a large linked void group constitutes a big void with an enhanced linking range. This enhancement occurs in uniaxial stress experiments done on sheets with drilled-in holes,[5-6], in which void clusters formed long, narrow structures perpendicular to the stress axis. The data[5] indicate that the linking range of a long, narrow void cluster extending perpendicular to the uniaxial strain is enhanced at the ends of the cluster, in the perpendicular direction, roughly by a factor equal to the square root of the cluster length.Thomason's approximate slip line solutions[4] can be used to deduce the square root law. In the 2D simulations done here, which involve uniaxial stress, the square root size enhancement will be used as a realistic approximation. The general results should not depend on the exact power.

2D PLANE STRAIN SIMULATIONS

In this section the 2D void link-up simulations and their results will be described. The applied stress used is uniaxial tension. No void nucleation is included. The growth of a random spatial distribution of equal-sized voids is studied. Wave propagation effects in the linking-up of voids are included in an approximate way.

Because of the uniaxial tension mostly long skinny void clusters will be produced, less so for the high strain rate case. This situation is not as restrictive as it might seem, because there is evidence, even for the quasi-static case,[2] that ductile void linking driven by more general stress fields occurs in 3D in sheets, or in 2D in narrow bands; in both cases, mostly perpendicular than not to the axis of greatest principle stress. For high strain rates, on the other hand, the void linking is much more uniform and random; its spatial pattern depends less on the triaxiality of the stress state. (The rate of individual void growth depends a great deal on the presence of negative pressure, however.)

The effects of local enhancements of void growth are not studied here for simplicity.

The action of stress release waves caused by a given growing cluster on nearby clusters has not yet been studied. The action of stress release waves from a cluster on the cluster itself is treated, of course, by means of the wave propagation modeling of void link-ups. This self action is responsible for the enhancement of void link up range.

The simulation results given include snapshots of the void arrays, the effect of strain rate on breaking strain, and the size effect of breaking.

The modeling of void linking range and void growth used here is reminiscent of that found for holes

in thin sheets by Magnusen et al.[5] We model general plastic loading, however, as so our results are appropriate for the case of 2D plane strain, which approximately includes 3D effects.

The simulations here are not hydrodynamic calculations in the usual sense. Stresses and strains are not calculated using the dynamic equations of motion with constitutive relations. Rather, a global uniform driving strain field is assumed, together with void growth laws and void link-up laws that are drawn qualitatively from experimental work like that of Magnusen et al[5], and slip line theory such as that of Thomason[2] and Melander and Stahlberg.[7,8] Hence, most of the physics enters into the calculation via the void growth and link up laws. The imposed uniform strain field is in the spirit of a "mean field theory" in which the local strain field seen by a cluster is an averaged imposed one. For this reason, the behavior will be predicted well only until the final breakup. This should suffice for constitutive modeling, however. Also, spatial variations in driving stress or strain are not treated; the results are suitable for a constant driving field as in a computational cell of a hydrocode.

For calculational simplicity, rectangles are used for the void shapes, instead of circles.

The void growth laws used are the following. The width of a void in the direction perpendicular to the stress axis stays at the constant value D_0. (The perpendicular direction will henceforth be referred to as the horizontal direction for brevity.) The height of a void, in the direction of the stress axis, grows as follows: $D = D_o(1 + \alpha e_1^a)$, where D_0 is the initial void size, e_1 is the longitudinal strain, and a and α are constants. The values used for a, α, and D_0 are 1.3 and 12.1 and 8.0×10^{-4}cm, respectively. Except for the value of D_o, they are reminiscent of the thin sheet results of Magnusen et al [5] for 1100-0 Al. Hence, the modeling here is typical of a soft metal with little workhardening and fairly vigorous void linking behavior. (Strong workhardening inhibits void linking.)The large void size is reminiscent of large inclusions. The law used for r, the link range of a void in the horizontal direction is as follows:

$r = D\sqrt{\frac{W}{D}}$, where W is the horizontal width of the cluster to which the void belongs. Thus, r is scaled by the void size. r is given the lower bound, D. As a consequence, the horizontal range of an isolated void is D. The link range of all voids in the direction along the stress axis is taken to be simply D/2[5]. The linking criteria is facilitated by constructing 'linking area figures' around each void, which in this case are rectangles centered on the void center of width 2r and height D. Two voids link when their linking figures overlap.

Stress wave propagation effects are introduced into the cluster size enhancement of the linking range by appropriately limiting the cluster width, W, used in the formula for r. Roughly speaking, W is bounded from above by C_l t. See Ref. [9] for more details. The idea is that a given void in a cluster will only "know about" other member voids if it is within the propagation distance of the release stress waves that originated when the other member voids linked up to their neighbors. The stress enhancement seen by a given void due to others in its cluster arises from the stress relaxation waves originating from the inter-void ligaments of the other voids when those ligaments failed or localized. It takes time for these relaxation waves to propagate. If not enough time has passed for such waves to travel along a cluster, a void in the cluster will not "see" the full width enhancement of its linking range. The value used for C_l was 4×10^5 cm/s.

Figures 1 and 2 show snapshots of the final, or breaking, void linking configuration for two simulations done at strain rates of 1/s and 10^7/s, respectively. The initial porosities are 0.05, and 4,000 voids were used. The initial void configurations are the same.

Except for the largest cluster, only rectangular outlines enclosing the void clusters are shown. For clusters with more than one void, the actual cluster outline falls inside this rectangle, as is seen for the largest cluster. For clusters with a single void, the outline is identical with the physical boundaries of the void. To provide more information, the largest cluster is broken down into individual void linking ranges (linking range figures).

The two crossed boxes along the axes in Fig. 2 are a ruler showing the wave propagation distance, $C_l t$. In Fig. 1, the ruler is longer than the system.

In Fig. 1, the void linking is not wave speed limited at the low strain rate of 1/s. The largest initial cluster rapidly overtook its fellows and broke the system. In the high strain rate simulation of Fig. 2, the initial situation was the same as for the quasistatic case. But in this case, the time evolution did not give rise to a single large crack because of the wave speed limitation of the cluster size range enhancement. Many clus-

ters grew large together, to break the system. At the end, there is a strong preference for long cluster shapes due to the uniaxial nature of the modeling, but the overlying randomness is also apparent.

The final strain at breaking for the high strain rate case is 0.197, significantly larger than that of 0.065 for the quasistatic case. This is because the damage was not organized into long, far reaching structures and, so, more of it had to occur until enough of it was present to break the system.

These two simulations illustrate well the transition from a quasi-static process in which the damage can organize and extend itself, to the high strain rate process in which the damage occurs almost randomly and finally breaks the system by simply overwhelming it everywhere.

This latter behavior, the high strain rate limit, is an example of random continuum site percolation theory.[10,11] In this theory, objects are placed at random and objects that overlap are said to be connected and to form clusters. When the biggest cluster spans the system, it breaks.

Percolation theory predicts that our systems should break when the quantity $2\langle r\rangle D\rho_o$, which we call Φ_p, reaches 1.1. This condition is realized fairly well at high strain rates, as we will shortly see.

Fig. 3 shows the breaking strain to failure for various initial porosities and strain rates, for a sample of size 0.832mm x 0.832mm. Various initial porosities imply differing numbers of voids. There were 3000, 2327, 1695, 1099, 813, 535, and 264 voids, ranging from the largest to the smallest initial porosity, for the initial porosities shown in Fig. 3. Note that the quasi-static curve involves the least strain to failure. The place where it intersects the x axis, at about 10% porosity, is the initial porosity at which failure will occur as soon as the stress waves have time to propagate and fail the nearest neighbor intervoid ligaments. (The initial porosity at which the system falls apart without ligament failure, i.e. simply by virtue of being full of holes, is at about 67%.) In general, the failure curves for higher strain rates fall at ever increasing strain. As mentioned earlier, this is because more strain with more random damage is necessary before the sample breaks when size enhancement of void linking is restricted by the requirements of the wave transit time. The curve portions that lie to the right of the static curve x-axis intercept, which involve higher strain rates, have non-zero strains to failure because some overall strain occurs while the stress waves are moving to cause the failure of the nearest neighbor intervoid ligaments.

Judging both by cluster morphology and the value of $2\langle r\rangle D\rho_o$, (which is Φ_p), the random percolation limit is approximated well for the curve in Fig. 3 with strain rate of 10^7/s and somewhat less well for the curve with strain rate of 10^6/s. The Φ_p values at breaking for the curve of strain rate 10^7/s, ranging from low to high initial porosity, were 1.070, 0.931, 0.921, 0.848, 0.970, 0.953, and 0.905, respectively. The 10^5/s strain rate curve involves one large breaking cluster except for initial porosities larger than 0.10, where percolation-like cluster morphology reappears. Here there is enough initial porosity for percolation like fracture as soon as the stress waves have time to reach out to nearby voids. The cluster morphology for the strain rate of 1/s always involved one large break.

The cluster size statistics were calculated for the simulations. They show a change from an exponential law at small strains, a sign of random clustering; to a power law at larger strains, which is a sign of organization. The change to a power law was also seen by Curtin and Scher in simulations in a different system.[12,13]

Fig. 4 shows, for the strain rate of 1/s, system size effects in quasi-static fracture, i. e. it shows $\rho_o D^2$, the "bare void porosity," at fracture versus the logarithm of the system size. The log of the system size seems to work fairly well here to straighten out the plotted line. This is similar to elastic beam systems.[14] The range in bare porosity is too small, however, to determine whether $\rho_o D^2$ or its logarithm produces a straighter curve.

Analytical Approximations

This section concerns certain analytical approximations to the 2D simulations. The emphasis will be on predicting the point of fracture. The analytical theory applies only qualitatively, but with adjustment of one parameter, it can predict the point of fracture of the simulations fairly well.

The basic analytical tool to be used here is an integral equation for the probability, P, that a given span in the horizontal direction (perpendicular to the tensile stress axis) is covered by a void cluster. By 'cover' is meant that the linking range of the cluster or the cluster itself covers the end of the interval. It is assumed that a seed void exists at the beginning of the span. A simpler quantity involving a constant link-

ing range is dealt with by Domb.[15]

The integral equation for P is as follows:

$$P(l) = \phi \int_{l_l}^{l} e^{-\phi (l - l')} P(l')\, dl' , \qquad (1)$$

where l is the horizontal distance (span) of the interval divided by D, the void size, and ϕ is the 'bare porosity' $\rho_o D^2$ times an adjustable factor, f. l_l, given by $l = l_l + \sqrt{l_l}$, is the smallest cluster length whose range covers the end of the interval with no intervening voids. The exponential is the probability that the intervening space is vacant. The integral is over all possible such cases.

The factor f was adjusted to obtain fits with the simulation results. It accounts for 2D effects like a a cluster wandering somewhat in the direction of the stress, as it grows horizontally. It should be at least two. An f-value of 5.5 was found to fit the quasi static simulation results.Thus, the 2D effects included through f are not trivial, but, with this f-value the 1D-like analytical theory is successful.

The calculated P is used to predict the breaking point in the following way. Each void in the system is taken to be a seed void which gives rise to a cluster family whose covering properties are given by P(l). The number of seeds is $L^2\rho_o$, where L is the system width. $L^2\rho_o$ times P(l), where l is L/D, is, thus, the probability that at least one of the seeds grows to a cluster that spans the system. Thus, when this expression equals one, the system should break. Only one direction of growth is assumed, which is appropriate for clusters almost as large as the system.

In Fig. 5 we have plotted P(l) and $1/(l^2\rho_o D^2)$ versus l. (Note that $l^2\rho_o D^2$ equals $L^2\rho_o$.) The intersection of the line with a curve for P(l) determines the l-value, or system size, that breaks for the given value of ϕ. Plots for several ϕ values are given to show the variation in breaking size with ϕ. The equation (1) was solved numerically.

The analytically calculated points in Fig. 4 were produced in this way. The trend of the simulation points there is fairly well reproduced by the calculation.

Wave propagation effects can be approximately introduced into the above theory by taking the lower bound in the integral equation to be the upper bound minus the minimum of the static range and the square root of $C_l t$. This has the effect for high strain rates, in the calculation of P(l), of eliminating the horizontal asymptote seen in Fig. 5 and producing a steep fall off, instead. The static type fracture mode is severely curtailed. The calculated P(l) can then be used to calculate a version of Φ_p, to see when it reaches 1.1 to predict when the percolation fracture mode takes over. This theory can roughly predict the percolation like fracture seen in the simulations with the same value of ϕ that predicts the static points of rupture. The X in Fig. 3 is a prediction for Φ_p using this approach.

Voronoi Tessellation with Application to Spallation

The Voronoi tessellation was been discovered to be of great help in describing ductile damage growth in 3D. In 3D, one can no longer rely on the void linking network to predict fracture like one can in 2D. In 2D, the creation of a spanning damage cluster coincides with the destruction of the network of solid that connects up the structure. In 3D, when a damage cluster spans the system, a network of solid still exists to hold it together. Somewhat more damage must be produced to break the spanning solid network. Hence, in 3D, the network of interconnecting solid must be considered in addition to the damage network. This is what the Voronoi tessellation does as well as giving the local details of linking.

For illustration purposes, Fig.6 shows a typical Voronoi tessellation in 2D. Each Voronoi edge represents a solid-connecting-ligament between voids. This ligament connects solid regions (an example of which is the "chunk" in the figure), that exist inside each triangle formed by three voids at the triangle corners. The Voronoi network, i. e. the ligaments, constitutes the interconnecting solid network which is eventually destroyed by void coalescence.

In 3D, the tessellation is constructed by forming the perpendicular bisecting planes to each void pair and then, for each void, selecting those planes that form an empty polygon about it. Each solid chunk is a tetrahedron with voids at the vertices. The connecting solid network can be thought of as lines extending, roughly, between the tetrahedral centers, which pack to fill the system. Each such connecting line runs perpendicularly through a gateway consisting of three voids arranged at the vertices of an equilateral triangle.

The line usually goes though the triangle near its center, but not always. The line can be thought of as a solid bond.

The breakup of the solid network occurs when these three gateway voids grow large enough to connect and make the solid connecting bond into a narrow neck. In this way, the solid constraint of the connecting bond is lost and it will very soon neck down and fail. This is the microscopic picture that the Voronoi tessellation provides of the internal damage mechanism. This mechanism provides a way for a negative pressure, say, to be turned into uniaxial tension within necks inside the sample; followed by rapid necking down and fracture.

So far, we have applied the tessellation to spallation under negative pressure, which involves the high strain rate percolation limit, described above. In rapid spallation, the void link up geometry will be isotropic, instead of directional as with uniaxial driving stress. Voids will have time only to link to their nearest neighbors. A continuous path of void will form in the system when ρV approximately equals 1.1, where ρ is the density of void centers and V is the volume (or average volume) of the 'linking volume figure'. (When the linking figures of two voids overlap, they link.)

In the 3D percolation calculation, identical voids were placed at random. The Voronoi tessellation was then performed to establish the pathways of the solid interconnecting network. The void size was increased in steps and the connectivity of the solid network examined after each step until no connection completely across the sample remained.

The solid bonds of the network, described above, were taken to fail immediately after a neck formed. In some cases, the three gateway voids are arranged such that no neck is possible. In these cases, the solid bond was taken to fail when these gateway voids had eaten away enough of the bond.

Under negative pressure, the immediate failure when a neck forms is reasonable for the following reasons. The action of the negative pressure on the neck is to suddenly throw the neck into a tension equal to the negative pressure. This magnitude of this tension will be very much greater than the yield stress, which is roughly the uniaxial stress that the neck can stand without failing by necking down. Thus, the neck rapidly fails by necking. This process can be viewed as a change in local geometry from 3D to 1D in which the large negative pressure that the material can support in 3D is changed to a large uniaxial stress that the neck cannot stand.

One adjustable modeling parameter, f, was used in the calculation, to determine the void linking radius as 1+f times the physical void radius. Plausible f-values range from 0.5 to 1.0. The value of f depends on the plastic workhardening. The f-values 1.0, 0.9, and 0.8 resulted in the breaking porosities 0.320, 0.375, and 0.442, respectively. The results follow closely the relation $\Phi_b=1-\exp(-\phi)$, where ϕ is $2.55/(1+f)^3$ and Φ_b is the breaking porosity.

As far as the author knows, this is the first theoretically correct 3-D percolation model for the spallation porosity in ductile materials. Most existing spall models use a porosity of about 0.30, based on the percolation of void spheres, which, as discussed above, is not the true spallation point. Depending on the workhardening, however, the value 0.30 could be roughly correct.

Acknowledgment

I am pleased to acknowledge support from the Joint DoD/DOE Munitions Technology Development Program and the DOE.

References.

1 Johnson J. N., J. Appl. Phys. 52 (1981) 2812.

2 Thomason P. F., *Ductile Fracture of Metals* (Pergamon, New York, 1990).

3 Thomason P. F., Acta Metall. *33* (1985) 1087.

4 Thomason P. F., J. Inst. of Metals 96 (1968) 360.

5 Magnusen P. E.,Srolovitz D. J., and Koss D. A., Acta Metall. Mater. *38* (1990) 1013.

6 Magnusen P. E., Dubensky E. M., and Koss D. A., Acta Metall. *36* (1988) 1503.

7 Melander A. and Stahlberg U., Int. J. Frac. *16* (1980) 431.

8 Melander A., Mat. Sci. Eng. *39* (1979) 57.

9 Tonks D. L., in Shock Compression of Condensed Matter IV, series ed. - Graham, volume editors - Davison, Grady, and Shahinpoor.

10 Stauffer D., *Introduction to Percolation Theory* (Taylor and Francis, London, 1985)

11 Balberg I., Anderson C. H., Alexander S., and Wagner N., Phys. Rev. *B30* (1984) 3933.

12 Curtin W. A. and Scher H., Phys. Rev. *B45* (1992-II) 2620.

13 , Curtin W. A. and Scher H., Phys. Rev. Lett. *67* (1991) 2457.

14 Sahimi M. and Arabi S., Phys Rev. *B47* (1993-II) 713

15 Domb C., *On Hammersley's Method for One-Dimensional Covering Problems* in *Disorder in Physical Systems*, edited by G. R. Grimmett and D. J. A. Welsh (Clarendon, Oxford, 1990).

Figure Captions

1 2D simulation snapshot for a strain rate of 1/s, i. e. quasistatic, at a breaking strain (e1) of 0.065. Localized damage.

2 2D simulation snapshot for a strain rate of 10^7/s and the breaking strain of 0.197. Percolation like damage.

3 Failure strain versus actual initial porosity at various strain rates. The squares, circles, triangles, and pluses are at strain rates of 1, 10^5, 10^6, and 10^7/s, respectively. The lines are to guide the eye. The X is a prediction of an analytic theory.

4 The squares are the logarithm of the system size (edge length) versus $\rho_o D^2$ at breaking for various systems. The circles are from the analytical approximation illustrated in Fig. 5. The line is to guide the eye.

5 Log log plot of P(l), the void covering probability for the interval of length l, versus l, for five actual porosities ranging from 0.087 to 0.123. The dotted line is an approximation to P(l) for the porosity 0.123. The straight line is a plot of $1/(l^2\rho_o D^2)$. The intercepts of this line with the solid curves gives the respective breaking sizes. Four of these are plotted in Fig. 4.

6 2D example of Voronoi tessellation showing solid interconnecting network (edges) and voids.

Fig. 1

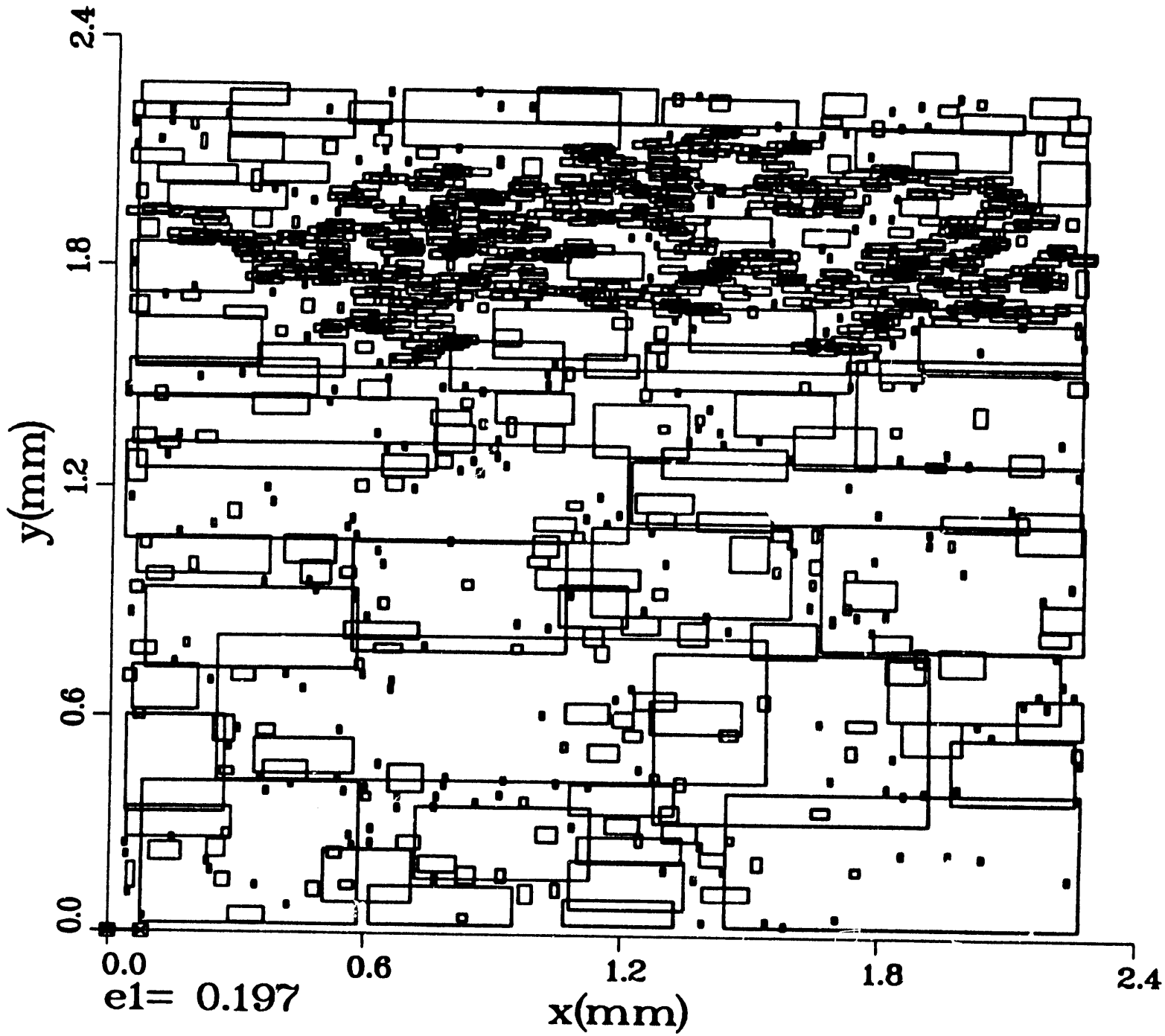

Fig.3a

e_f(failure strain)
0.00 0.05 0.10 0.15 0.20 0.25 0.30 0.35
0.00
0.05
0.10
0.15
0.20
0.25
φ_o(init porosity)

Fig. 3.

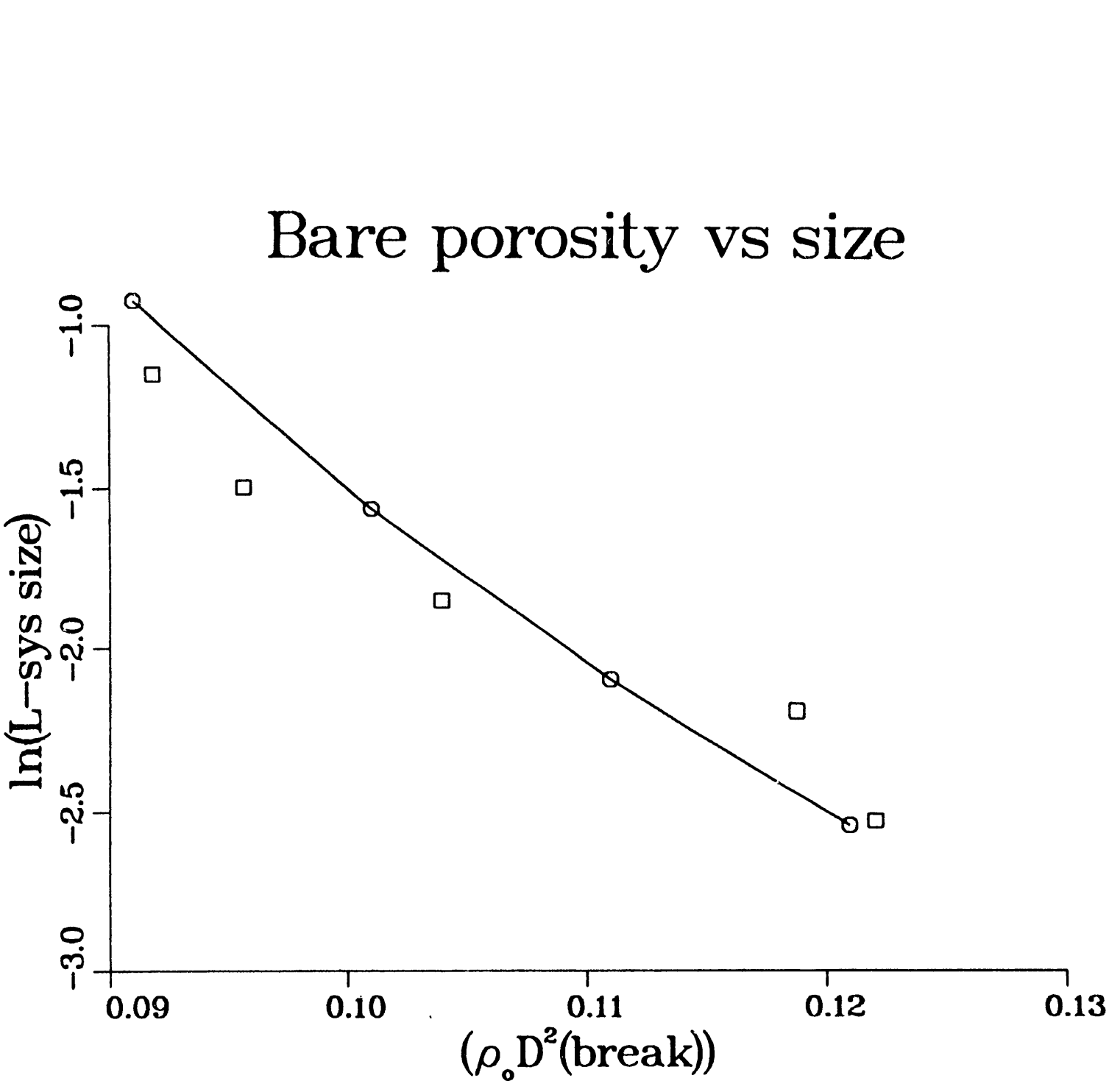
Bare porosity vs size
ln(L–sys size)
-1.0
-1.5
-2.0
-2.5
-3.0
0.09
0.10
0.11
0.12
0.13
($\rho_o D^2$(break))

Fig. 11

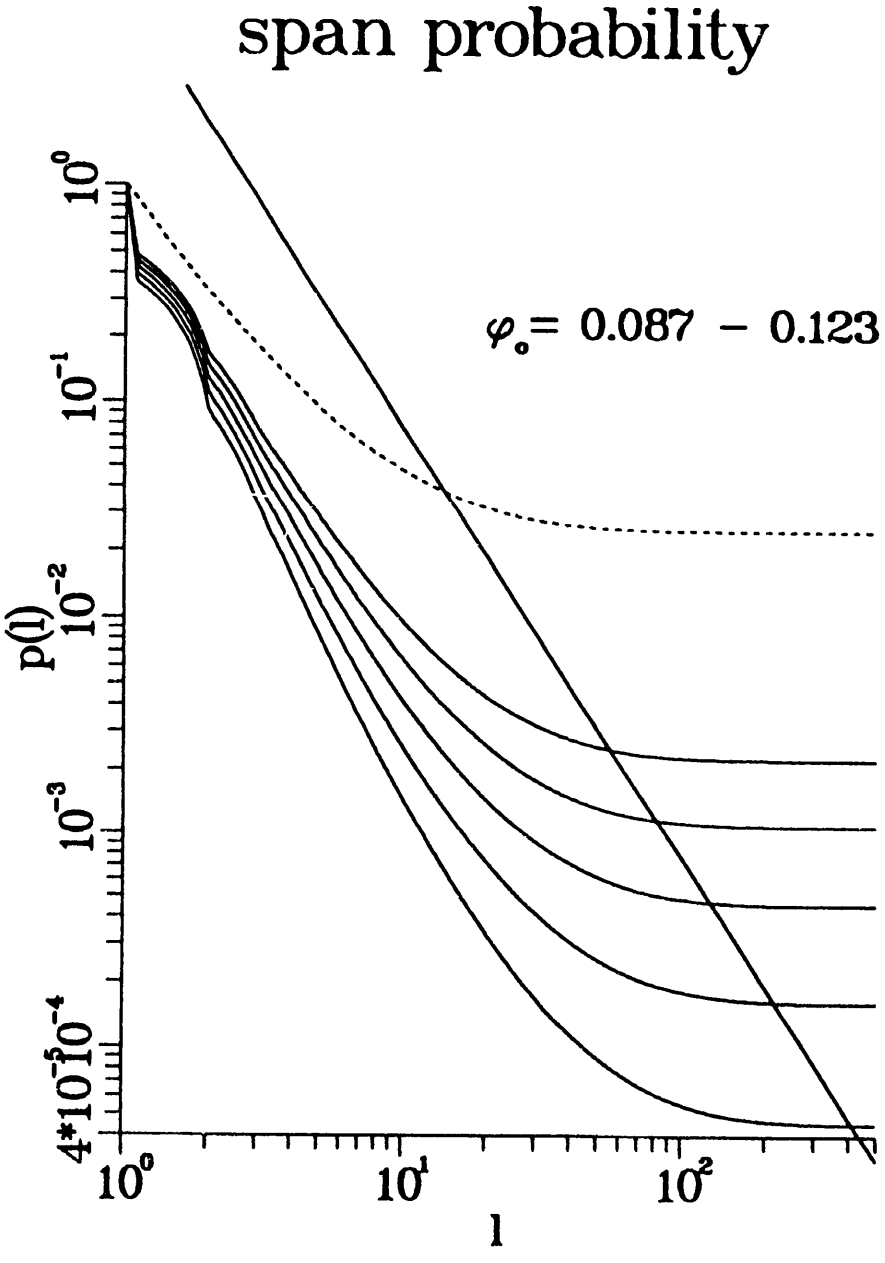
span probability
φ_o= 0.087 – 0.123
p(l)
l
10^0
10^{-1}
10^{-2}
10^{-3}
$4*10^{-3}$
10^{-4}
10^0
10^1
10^2

Fig. 5

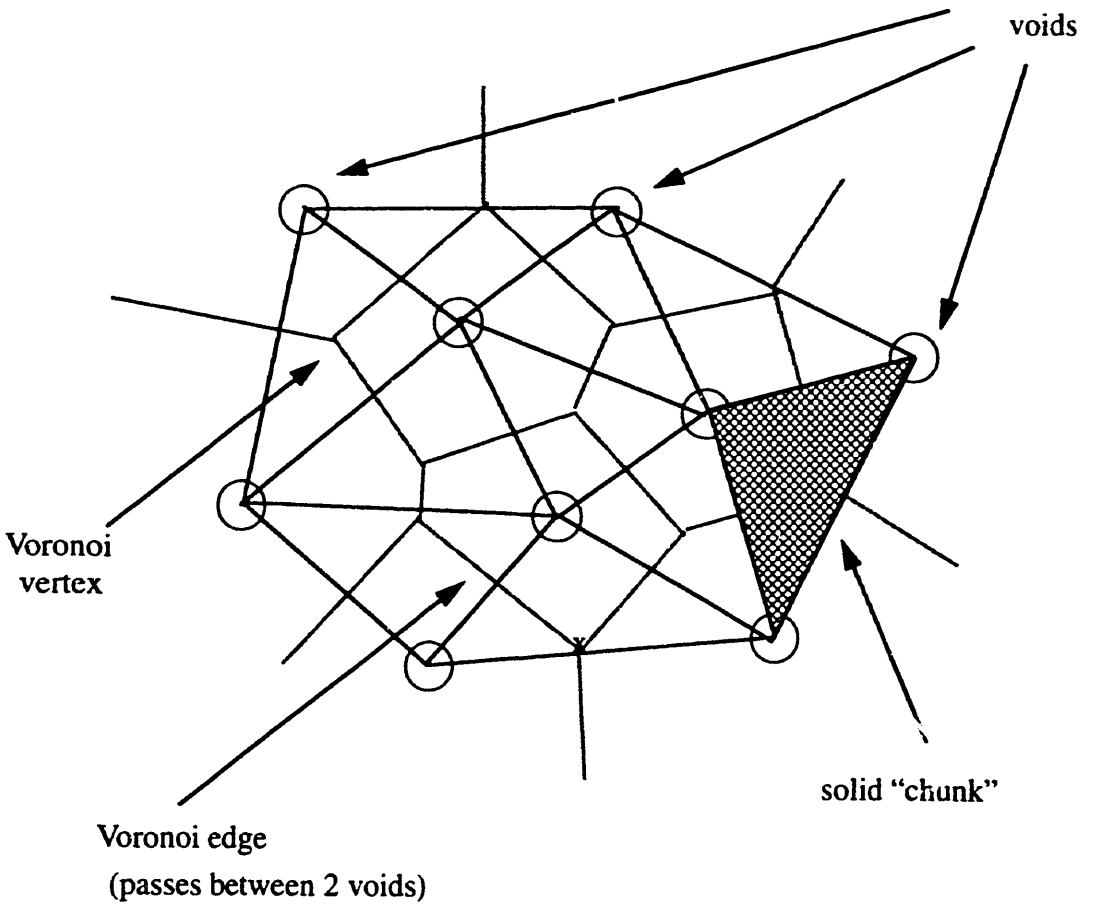
voids
Voronoi
vertex
solid "chunk"
Voronoi edge
(passes between 2 voids)

Fig. 6

DATE
FILMED
8/4/94

END